

Myotendinous Junctions

Subjects: Biology

Contributor: Lara Rocha

The myotendinous junction (MTJ) is the muscle-tendon interface and constitutes an integrated mechanical unit to force transmission. Joint immobilization promotes muscle atrophy via disuse, while physical exercise can be used as an adaptative stimulus. In this study, we aimed to investigate the components of the MTJ and their adaptations and the associated elements triggered with aquatic training after joint immobilization. Forty-four male Wistar rats were divided into sedentary (SD), aquatic training (AT), immobilization (IM), and immobilization/aquatic training (IMAT) groups. The samples were processed to measure fiber area, nuclear fractal dimension, MTJ nuclear density, identification of telocytes, sarcomeres, and MTJ perimeter length. In the AT group, the maintenance of ultrastructure and elements in the MTJ region were observed; the IM group presented muscle atrophy effects with reduced MTJ perimeter; the IMAT group demonstrated that aquatic training after joint immobilization promotes benefits in the muscle fiber area and fractal dimension, in the MTJ region shows longer sarcomeres and MTJ perimeter. We identified the presence of telocytes in the MTJ region in all experimental groups. We concluded that aquatic training is an effective rehabilitation method after joint immobilization due to reduced muscle atrophy and regeneration effects on MTJ in rats.

Keywords: nuclear domain ; sarcomere ; telocyte ; muscle-tendon perimeter ; aquatic training ; joint immobilization

1. Introduction

The myotendinous junction (MTJ) anchors the terminal sarcomeres to the extracellular matrix (ECM). The MTJ is the site of contractile force transmission from the muscle to the tendon, and the higher contact area between the muscle and tendon provides resistance to the muscle contractile force ^[1].

Joint immobilization promotes inactivity, which leads to muscle atrophy via disuse. Moreover, joint immobilization promotes diverse deleterious effects in the post-immobilization period in the form of impaired muscle performance ^[2] and reduced myotendinous interface ^{[3][4]}.

Muscle fibers in normal conditions contain multiple nuclei that are peripherally organized. However, in communicating junctions (such as MTJ), the nuclear position is specialized and demonstrates adaptations associated with mechanical stimulus ^[5].

Recently, a study identified telocytes as a new element that are adjacent to MTJ ^[6] in the interstitium. They are characterized by telopods (long and thin projections) and pods (dilated segments) with mitochondria and endoplasmic reticulum ^[7]. The telopods establish communication and paracrine activity that help different cell types interact, including blood vessels, nerve cells, immune cells, fibrocytes, stem cells, granular cells, and others, under normal and pathological conditions ^{[7][8][9]}.

The period after joint immobilization is a critical period toward recovery as well as for the mitigation of deleterious effects in muscle fibers and postsynaptic components ^[10]. Alterations in the ligand proteins of ECM, laminin, and dystrophin in the post-immobilization period ^[11] reduce the extensibility and plasticity properties of muscle fibers, rendering them susceptible to muscle injuries. However, stimulus in the form of physical activity revealed positive responses to these characteristics ^{[12][13]}.

In the present study, we investigated the components of the MTJ and their adaptations as well as the associated elements that are triggered following aquatic training (AT) after joint immobilization.

2. Aquatic Training after Joint Immobilization in Rats Promotes Adaptations in Myotendinous Junctions

2.1. Fiber Area

The AT group had a lower fiber area than the SD group ($p = 0.0001$). The IM group had a lower fiber area than the SD group ($p < 0.0001$) and AT groups ($p < 0.0001$). By contrast, the IMAT group had a lower fiber area than the SD group ($p = 0.0001$) and a higher fiber area than the IM group ($p < 0.0001$) (**Figure 1**).

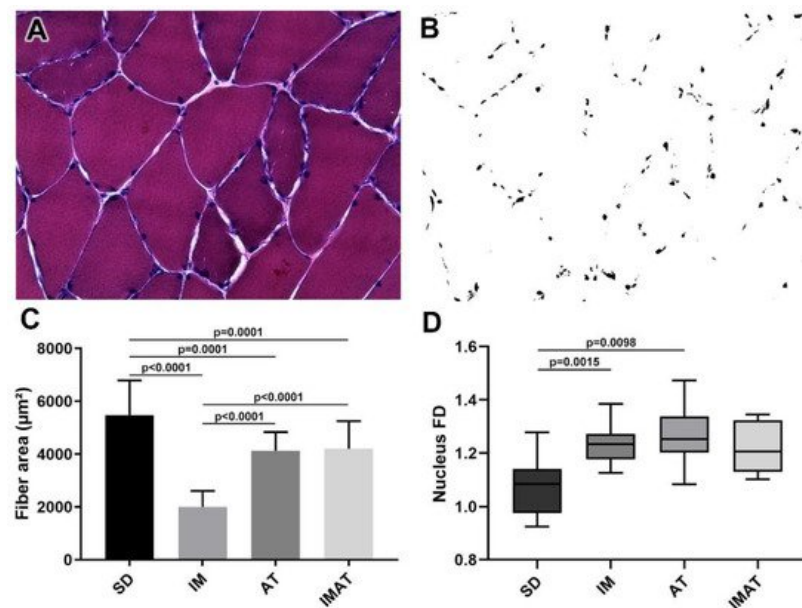


Figure 1. Analysis of muscle fibers of the belly of gastrocnemius muscle of Wistar rats. **(A)** Light microscopy of belly muscle in hematoxylin-eosin staining (HE), magnification: 400 \times . **(B)** Binarized image of HE staining with nucleus highlight for fractal dimension (FD) analysis. **(C)** Mean \pm standard deviation of muscle fibers area (μm^2) of sedentary (SD), immobilization (IM), aquatic training (AT), and immobilization/aquatic training (IMAT); SD \neq AT ($p = 0.0001$), SD \neq IM ($p < 0.0001$), SD \neq IMAT ($p = 0.0001$), AT \neq IM ($p < 0.0001$), and IM \neq IMAT ($p < 0.0001$). **(D)** Box plot of nucleus FD analysis of groups; SD \neq AT ($p = 0.0015$) and SD \neq IM ($p = 0.0098$).

2.2. Fractal Dimension (FD)

The AT ($p = 0.0015$) and IM ($p = 0.0098$) groups had a higher FD than the SD group (**Figure 1**).

2.3. MTJ Nuclear Density

The IM group had a lower MTJ nuclear density than the AT ($p = 0.0002$) and IMAT ($p = 0.0005$) groups. The other groups showed no significant difference (**Figure 2**).

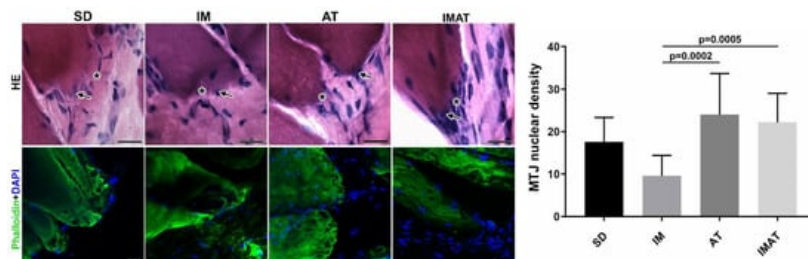


Figure 2. Light microscopy of hematoxylin-eosin staining (HE) of MTJ (*) and adjacent nucleus (arrow) of sedentary (SD), immobilization (IM), aquatic training (AT), and immobilization/aquatic training (IMAT) from gastrocnemius muscle of Wistar rats. Bars: 20 μm . Immunohistochemistry of MTJ region of F-actin (Phalloidin) and nucleus (DAPI). Bars: 20 μm . Mean \pm standard deviation of MTJ nuclear density (unity/91.3 mm²) of groups; AT \neq IM ($p = 0.0002$) and IM \neq IMAT ($p = 0.0005$).

2.4. MTJ Morphology

Through the ultrastructural descriptions of the MTJ, its morphology and plasticity as well as associated elements were revealed, i.e., telocytes (**Figure 3**). We observed branched sarcoplasmic invaginations and a telocyte surrounding the

MTJ near a blood capillary in the SD group.

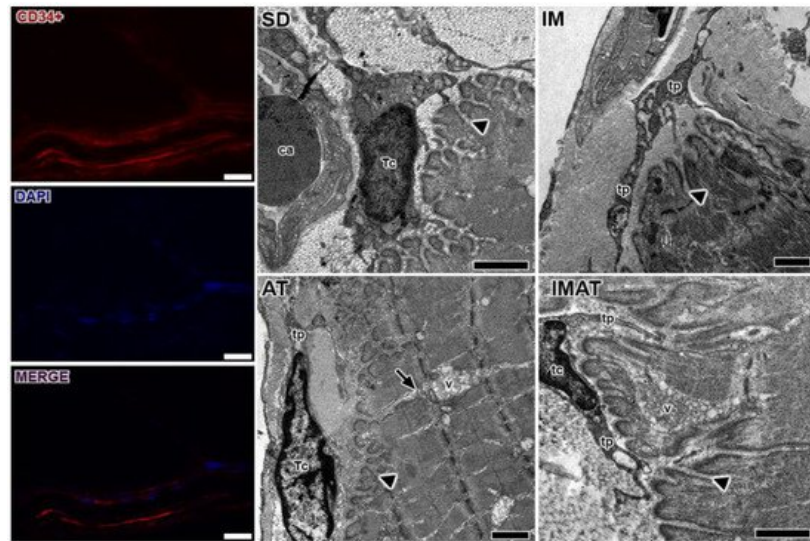


Figure 3. Telocytes analysis of MTJ region with immunostaining (CD34+), nucleus (DAPI), and the image with associated elements (MERGE). Bars: 20 µm. Transmission electron microscopy of MTJ of sedentary (SD), immobilization (IM), aquatic training (AT), and immobilization/aquatic training (IMAT) from gastrocnemius muscle of Wistar rats. In the myotendinous region the presence of blood capillary (ca) and telocyte (tc) with their projections the telopods (tp) is observed; these elements were observed adjacent to sarcoplasmic invaginations (arrowhead), and in the AT group a prolonger branch of sarcoplasmic invagination (arrow) with association with a vesicle group (v) is observed. Bars: 1 µm.

In the IM group, we observed a few sarcoplasmic projections and the presence of telopods near the MTJ as well as a centralized myonucleus in the muscle fiber close to the MTJ (**Figure 4**). In the AT group, we observed branched sarcoplasmic invaginations, the presence of a telocyte in ECM and their telopods, and a long sarcoplasmic invagination connected to a vesicle cluster inside the muscle fiber. Compared with the AT group, the IMAT group had longer sarcoplasmic projections in addition to telocyte and their associated telopods and a vesicle cluster inside the muscle fiber.

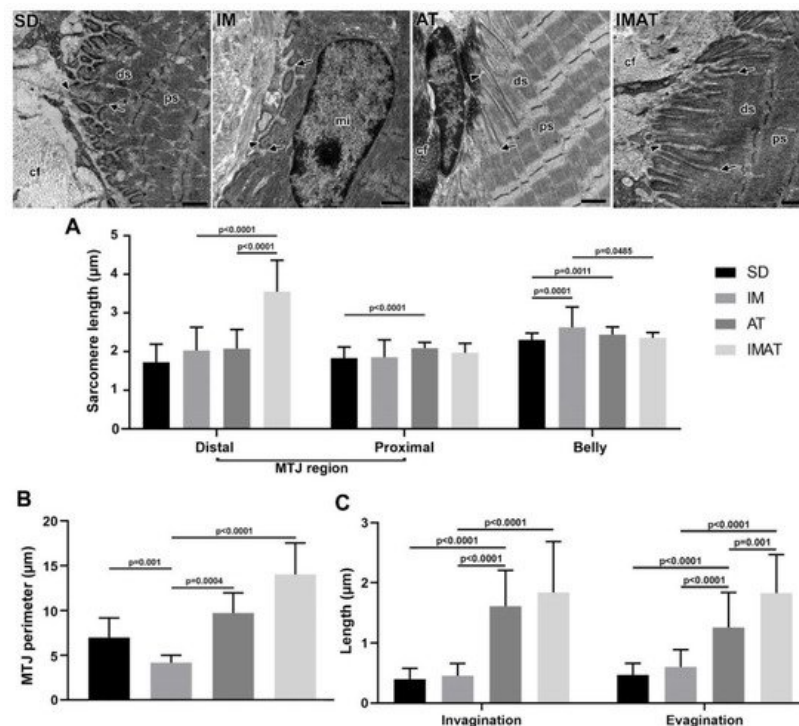


Figure 4. Transmission electron microscopy of MTJ region of sedentary (SD), immobilization (IM), aquatic training (AT), and immobilization/aquatic training (IMAT) from gastrocnemius muscle of Wistar rats. In the ECM collagen fibers (cf) organized in transversal and longitudinal form were observed, as well as the sarcoplasmic invaginations (arrowhead) and evaginations (arrow) associated to distal (ds) and proximal (ps) sarcomeres; in IM group a centralized myonucleus (mi) in the muscle fiber was observed. Bars: 1 µm. (A) Mean \pm standard deviation of sarcomere length (µm) localized in the MTJ region, distal and proximal, and of the belly muscle of groups; distal sarcomere: IM and AT \neq IMAT ($p < 0.0001$);

proximal sarcomere: SD \neq AT ($p < 0.0001$); belly sarcomere: IM \neq SD ($p = 0.0001$), AT \neq SD ($p = 0.0011$), and IM \neq IMAT ($p = 0.0485$). **(B)** Mean \pm standard deviation of MTJ perimeter determined in the contact area of 2 μm between sarcoplasmic invagination and evagination of groups; SD \neq IM ($p = 0.001$), AT \neq IM ($p = 0.0004$), and IM \neq IMAT ($p < 0.0001$). **(C)** Mean \pm standard deviation of length of sarcoplasmic invagination and evaginations of groups; invaginations: AT \neq SD ($p < 0.0001$), AT \neq IM ($p < 0.001$), and IMAT \neq IM ($p < 0.0001$); evaginations: AT \neq SD ($p < 0.0001$), AT \neq IM ($p < 0.0001$), IMAT \neq IM ($p < 0.0001$), and IMAT \neq AT ($p = 0.001$).

2.5. Sarcomeres

The distal sarcomere had longer lengths in the IMAT group than in the IM ($p < 0.0001$) and AT groups ($p < 0.0001$). The AT group had longer proximal than the SD group ($p < 0.0001$). The belly sarcomeres were longer in the IM group than in the SD ($p = 0.0001$) and IMAT groups ($p = 0.0485$); the AT group had longer sarcomeres than the SD group ($p = 0.0011$) (**Figure 4**).

2.6. MTJ Morphometry

The IM group demonstrated a shorter MTJ perimeter than the SD ($p = 0.001$) and AT ($p = 0.0004$) groups. By contrast, the lengths of sarcoplasmic invagination and evagination in the IM group were not significantly different from the SD group ($p > 0.05$) but were lower than the AT ($p < 0.0001$) and IMAT ($p < 0.0001$) groups.

The AT group showed a higher MTJ perimeter than the IM group ($p = 0.0004$). Moreover, the AT group had longer sarcoplasmic invagination and evagination lengths than the SD ($p < 0.0001$) and AT groups ($p < 0.0001$).

The IMAT group had longer MTJ perimeter ($p < 0.0001$) and longer sarcoplasmic ($p < 0.0001$) invaginations than the IM group. In addition, the IMAT group had longer sarcoplasmic evaginations than the IM ($p < 0.0001$) and AT groups ($p = 0.001$) (**Figure 4**).

3. Discussion

The results of this study revealed the joint immobilization effect of muscle atrophy due to disuse. The study also showed the effect and repercussion of AT as a rehabilitation method for the muscle belly and the muscle-tendon complex as well as other parameters, including the nucleus, sarcomere, contact perimeter, and telocyte.

References

1. Ciená, A.P.; Luques, I.U.; Dias, F.J.; Yokomizo de Almeida, S.R.; Iyomasa, M.M.; Watanabe, I.S. Ultrastructure of the myotendinous junction of the medial pterygoid muscle of adult and aged Wistar rats. *Micron* 2010, 41, 1011–1014.
2. Natali, L.H.; da Silva, T.S.; Ciená, A.P.; Padoin, M.J.; Alves, É.P.B.; Aragão, F.A.; Bertolini, G.R.F. Efeitos da corrida em esteira em músculos sóleos de ratos encurtados por imobilização. *Rev. Bras. Med. Do Esporte* 2008, 14, 490–493.
3. Kannus, P.; Jozsa, L.; Kvist, M.; Lehto, M.; Jarvinen, M. The effect of immobilization on myotendinous junction: An ultrastructural, histochemical and immunohistochemical study. *Acta Physiol. Scand.* 1992, 144, 387–394.
4. Curzi, D. Ultrastructural study of myotendinous junction plasticity: From disuse to exercise. *Sport Sci. Health* 2016, 12, 279–286.
5. Perillo, M.; Folker, E.S. Specialized Positioning of Myonuclei Near Cell-Cell Junctions. *Front. Physiol.* 2018, 9, 1–10.
6. Pimentel Neto, J.; Rocha, L.C.; Barbosa, G.K.; Jacob, S.; Krause Neto, W.; Watanabe, I.; Ciená, A.P. Myotendinous junction adaptations to ladder-based resistance training: Identification of a new telocyte niche. *Sci. Rep.* 2020, 10, 1–8.
7. Popescu, L. Telocytes-a novel type of interstitial cells. *Recent Res. Mod. Med.* 2011, 11, 424–432.
8. Edelstein, L.; Fuxe, K.; Levin, M.; Popescu, B.O.; Smythies, J. Telocytes in their context with other intercellular communication agents. *Semin. Cell Dev. Biol.* 2016, 55, 9–13.
9. Marini, M.; Rosa, I.; Ibba-Manneschi, L.; Manetti, M. Telocytes in skeletal, cardiac and smooth muscle interstitium: Morphological and functional aspects. *Histol. Histopathol.* 2018, 33, 1151–1165.
10. Rocha, L.C.; Jacob, C.d.S.; Barbosa, G.K.; Neto, J.P.; Neto, W.K.; Gama, E.F.; Ciená, A.P. Remodeling of the skeletal muscle and postsynaptic component after short-term joint immobilization and aquatic training. *Histochem. Cell Biol.* 2020, 154, 621–628.

11. Cação-Benedini, L.O.; Ribeiro, P.G.; Prado, C.M.; Chesca, D.L.; Mattiello-Sverzut, A.C. Immobilization and therapeutic passive stretching generate thickening and increase the expression of laminin and dystrophin in skeletal muscle. *Braz. J. Med. Biol. Res.* 2014, 47, 483–491.
12. Carvalho, L.C.; Polizello, J.C.; Padula, N.; Freitas, F.C.; Shimano, A.C.; Mattiello-sverzut, A.C. Mechanical properties of gastrocnemius electro stimulated after immobilization. *Acta Ortop Bras* 2009, 17, 269–272.
13. Cação-Benedini, L.O.; Ribeiro, P.G.; Gomes, A.R.S.; Ywazaki, J.L.; Monte-Raso, V.V.; Prado, C.M.; Mattiello-Sverzut, A.C. Remobilization through stretching improves gait recovery in the rat. *Acta Histochem.* 2013, 115, 460–469.

Retrieved from <https://encyclopedia.pub/entry/history/show/28756>